Influence of the Flowing Conditions on the Galvanic Corrosion of the Copper/AISI 304 Pair in Lithium Bromide Using a Zero-Resistance Ammeter

M.T. Montañés, R. Sánchez-Tovar, J. García-Antón[*], V. Pérez-Herranz

Ingeniería Electroquímica y Corrosión (IEC)
Departamento de Ingeniería Química y Nuclear. E.T.S.I.Industriales
Universidad Politécnica de Valencia, E-46022 Valencia. Spain
[*]E-mail: jgarciaa@iqn.upv.es

In this work, the influence of Reynolds number (Re) on the galvanic corrosion of the copper/AISI 304 stainless steel pair in an 850 g/L lithium bromide solution was evaluated in a hydraulic circuit using a zero-resistance ammeter; this technique has the advantages that it can be used without disturbing the system under investigation and in continuous-time. Results show that copper is the anodic member of the pair for all the Re analyzed. The galvanic current density values are always greater under flowing than under stagnant conditions. A general tendency of galvanic current density to decrease with time is observed due to the formation of a film of corrosion products on copper surface. Under flowing conditions, initially, galvanic current density increases with Re; however, with time, this tendency is reversed. As Re increases, greater quantities of corrosion products are initially produced and, as a result, a thicker film is formed.

1. INTRODUCTION

Nowadays, very few works have studied the galvanic corrosion process under flowing conditions [1-7]. Additionally, these studies have used rotating electrodes in order to simulate a hydrodynamic regime, but these electrodes do not effectively simulate what really occurs in the industrial environment of interest. As electrochemical measurements are commonly used to evaluate galvanic corrosion, in this work a hydraulic circuit was used to study the corrosion under flowing conditions *in situ* by means of electrochemical measurements without altering pipe continuity.

Although galvanic corrosion is usually investigated by the analysis of potentiodynamic polarization curves according to the mixed potential theory [8, 9], the quantitative data obtained by this method may be critically analysed because the polarization applied can cause irreversible disturbances in the system parameters. Another electrochemical measurement consists of the use of a zero-resistance ammeter (ZRA) to register the naturally occurring fluctuations in the potential and current of corroding electrodes that take place during a corrosion process [10]. Currently, the use of this technique is gaining importance because it has the advantages that it can be used without disturbing the system under investigation and in continuous-time [11]. Moreover, the analysis of the ZRA measurements makes it possible to determine the corrosion mechanism and the corrosion rate [12]. As it is a non-destructive technique, it can be expected that the results obtained will be very close to reality.

Few works have used a zero-resistance ammeter to evaluate corrosion under hydrodynamic conditions and most of them have studied the corrosion of a single metal, usually stainless steel; however, the presence of another metal, e.g. copper, which can produce galvanic corrosion, has not been considered [13-15]. Kear used a zero-resistance ammeter to evaluate the galvanic corrosion between copper and bronze and between stainless steel and bronze in seawater by using a bimetallic rotating cylinder electrode [6, 7]. Mansfeld used a zero-resistance ammeter to evaluate the galvanic corrosion between different materials (copper, stainless steel, aluminium and titanium) in substitute ocean water by using an electrode holder which contained dissimilar metals [1-3]. There is a lack of works which analyse galvanic corrosion using a zero-resistance ammeter, as some authors have indicated [16].

Absorption cooling is a suitable alternative to refrigeration compression systems because the use of chlorofluorocarbons (CFCs) has been banned (Montreal Protocol [17], 1987) and their substitutes, i.e. hydrochlorofluorocarbons, are submitted to severe regulations (Kyoto Protocol [18], 1997), since they are responsible for the ozone layer depletion and the climate change. Moreover, solar energy, which is available in hot climates, could be used to power an active cooling system based on the absorption cycle in order to contribute to the rational utilisation of energy and the protection of the environment. Lithium bromide (LiBr)-water absorption units are the most suitable for solar applications, since low cost solar collectors may be used to power the generator of the machine [19, 20]. However, despite the favourable thermophysical properties of lithium bromide [21, 22], it contains bromides which are aggressive ions and, thus, they can cause serious corrosion problems [23]. The high temperatures and concentrations reached in absorption machines may accelerate the corrosion effect of bromides. Additionally, the fluid flow can enhance these corrosion problems [24-26]. Besides this, absorption machines are constructed with different materials; therefore, the formation of galvanic pairs may accelerate the corrosion problems.

Copper and stainless steels are commonly used in the construction of absorption machines [19]. Specifically, copper is widely used in heat exchanger piping [27-30] and AISI 304 stainless steel is commonly used in the structural elements. Thus, AISI 304 stainless steel could cause important corrosion damage on copper in absorption machines due to galvanic effects. Galvanic corrosion between steels and copper has been studied in different environments, e.g. cooling water [31], sodium chloride [32] or sea-water [33]; however, none of these works has used concentrated LiBr solutions.

The purpose of the present work was to investigate the effect of the Reynolds number on the galvanic corrosion of the copper/AISI 304 stainless steel pair in an 850 g/L LiBr solution (commercial heavy brine LiBr solutions used in absorption machines) by using a zero-resistance ammeter (ZRA) in a hydraulic circuit. The experiments were carried out for a range of Reynolds numbers from 633 to 5066 during 24 hours. The stagnant conditions were also studied to simulate the possible stops of the absorption machines, due to maintenance and mechanical failure.

2. MATERIALS AND METHODS

2.1. Flowing conditions

Figure 1 shows a schematic diagram of the hydraulic circuit used for the experiments. It consisted of a centrifugal pump, a flow-meter, a thermostat to regulate the solution temperature, a valve to drain the system, and several glass devices: for the reference electrode, for a thermometer to control the temperature, to introduce the solution into the flow circuit and to bubble an inert gas; silicone flexible tubes were used to assemble the different elements. The test section was composed of two rings 20 mm in length and 14 mm in inner diameter, made of AISI 304 stainless steel (located at the flow inlet) and copper, respectively; they were insulated by a Teflon intermediate assembly piece which was 14 mm in inner diameter too. The reference electrode was placed at the flow outlet of the test section. Fully developed flow was assured using a 90-cm-long Teflon rigid tube of the same inner diameter as the test rings upstream of the test section and a 20-cm-long Teflon rigid tube downstream of the test section.
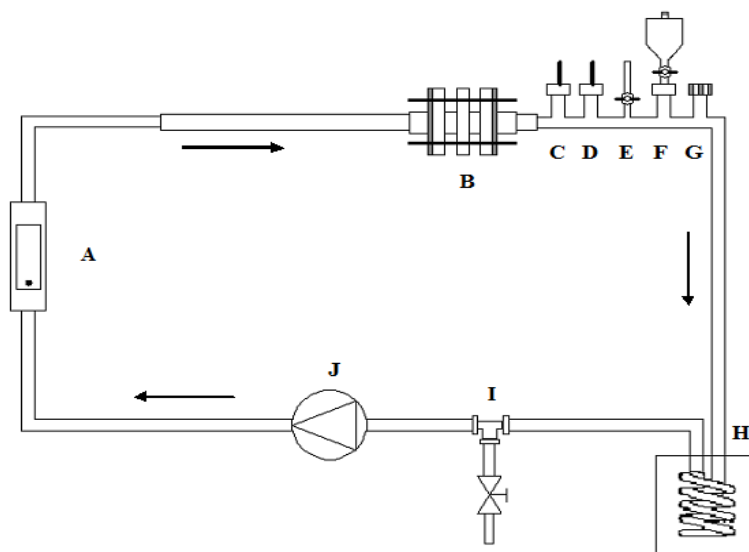

Figure 1. Schematic diagram of the hydraulic circuit used for the experiments. A: flow-meter, B: test section, C: glass device for the reference electrode, D: glass device for the thermometer to control the temperature, E: glass device for the gas output, F: glass device to introduce the solution into the flow circuit, G: glass device to bubble in an inert gas, H: thermostat, I: valve to drain the system and J: centrifugal pump.

Three flow rates were analysed: 73, 365 and 584 L/h, which were equivalent to fluid velocities 0.13, 0.66 and 1.05 m/s, respectively, and to Reynolds numbers 633, 3166 and 5066, respectively. The Reynolds number (Re) is a dimensionless group defined as:

$$Re = \frac{v \cdot d \cdot \rho}{\mu} \tag{1}$$

where v is the characteristic fluid velocity, d is the characteristic length of the system (the diameter of a pipe in the case of pipe flow), ρ is the fluid density and μ is the fluid viscosity. The LiBr solution density and viscosity were experimentally obtained in order to calculate the Reynolds number; the values obtained were 1.59 g/cm^3 and 4.64 Cp, respectively. Stagnant conditions were also analysed.

The experiments were carried out at 25 ºC.

2.2. Materials and solution

The copper and AISI 304 stainless steel rings were used in their as-received conditions [34]. They were only degreased with acetone, air-dried and weighed prior to exposure. Copper purity was 99.9 wt.% and Table 1 shows the composition of the AISI 304 stainless steel used in this work. After each experiment, the test section was disassembled and the rings were washed with distilled water, rinsed with acetone, air-dried and weighed again. Then, they were cut in order to observe their internal surface.

Table 1. Composition (wt.%) of AISI 304 stainless steel used in this work according to the inspection certificate supplied by the manufacturer.

C	Cr	Ni	Mn	Si	S	P	Fe
0.040	18.080	8.030	1.210	0.300	0.001	0.027	Bal.

The test solution was prepared by dissolving reagent grade LiBr in distilled water. Its concentration was 850 g/L and its pH was 10 like in the commercial solutions commonly used in absorption machines. Nitrogen was bubbled into the solution during 60 minutes to simulate oxygen-absence conditions in these machines, according to ASTM G5 [35]. Moreover, nitrogen was also bubbled when the solution was inside the hydrodynamic circuit during 20 minutes thanks to the glass device located in the hydraulic circuit for this purpose (see Figure 1, G). Then, the hydrodynamic circuit was completely closed to keep these conditions.

2.3. Electrochemical measurements

The electrochemical measurements have been performed using a zero-resistance ammeter (ZRA). Copper and AISI 304 stainless steel were connected to a Solartron 1285 potentiostat, which was used as a ZRA. Figure 2 shows a schematic diagram of the electrical connections carried out. Copper was connected to the working electrode (WE) terminal of the potentiostat, AISI 304 stainless steel was connected to the earth terminal (grounded) of the potentiostat and a silver/silver chloride (Ag/AgCl), 3M potassium chloride (KCl) electrode was connected to the reference electrode 1 (RE1) terminal of the potentiostat. Moreover, a short-circuit was established between the WE terminal and the reference electrode 2 (RE2) terminal of the potentiostat [36]. These electrical connections allow us to measure the current between both copper and AISI 304 stainless steel and their galvanic potential with respect to the reference electrode. The galvanic current and potential established between the pairs were measured every 0.5 s during 24 h. As the potentiostat measures current coming from WE terminal, the current sign was positive when electrons flowed from copper to WE terminal; thus, copper was corroding, because it lost electrons. Current values were negative when the electrons flowed in the opposite direction, that is, AISI 304 stainless steel was corroding. In all cases, the tests were repeated at least three times in order to verify reproducibility.
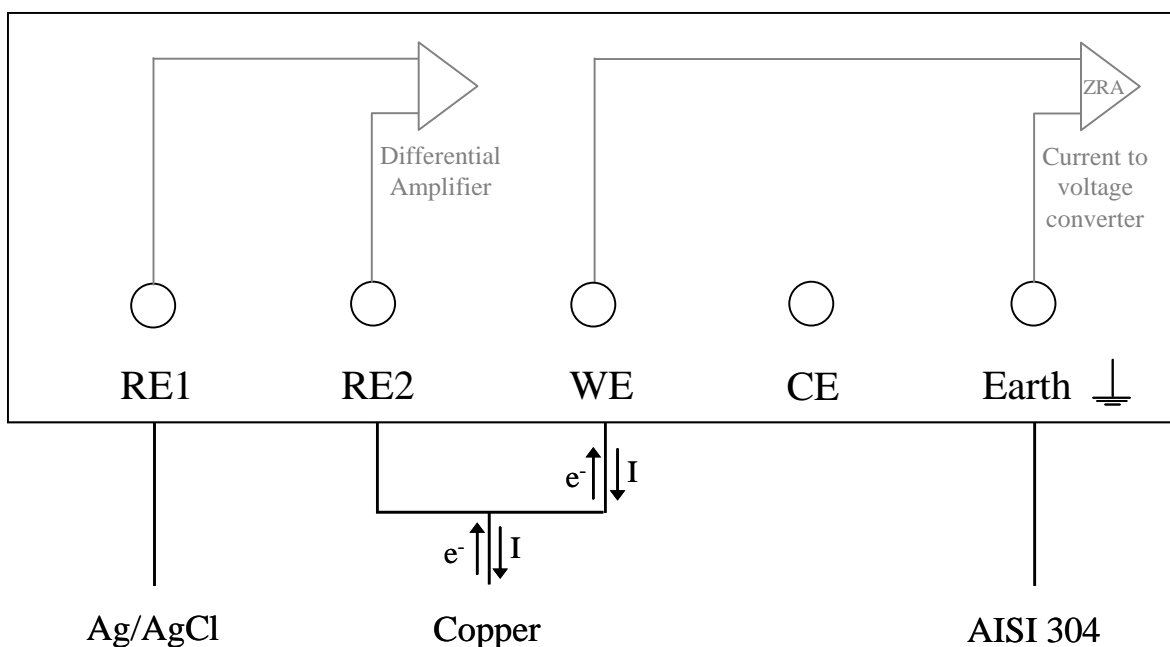

**Figure 2.** Schematic diagram of the electrical connections used in the tests.

The electrochemical measurements were analysed by visual inspection of the signals registered with time. On the other hand, the statistical analysis of signal fluctuations served to obtain the localization index [12]; this parameter can be used to obtain qualitative information about the corrosion mechanism.
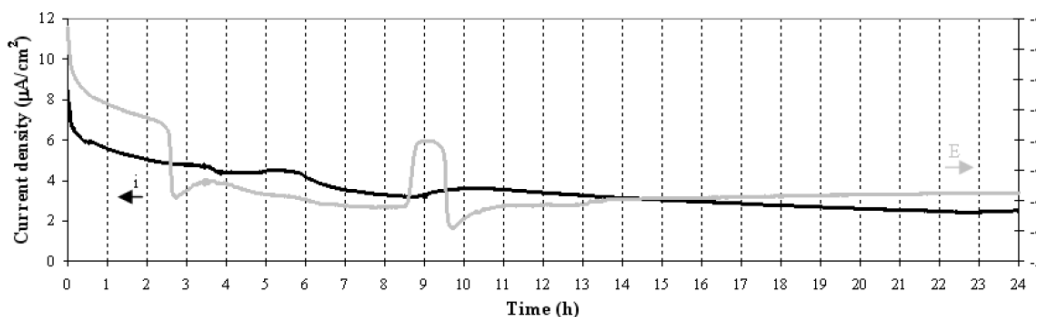
3. RESULTS AND DISCUSSION

3.1. Galvanic current density and galvanic potential profiles examination

Figure 3 shows the galvanic current density and the galvanic potential profiles of the copper/AISI 304 stainless steel pair during 24 h at different Reynolds numbers.
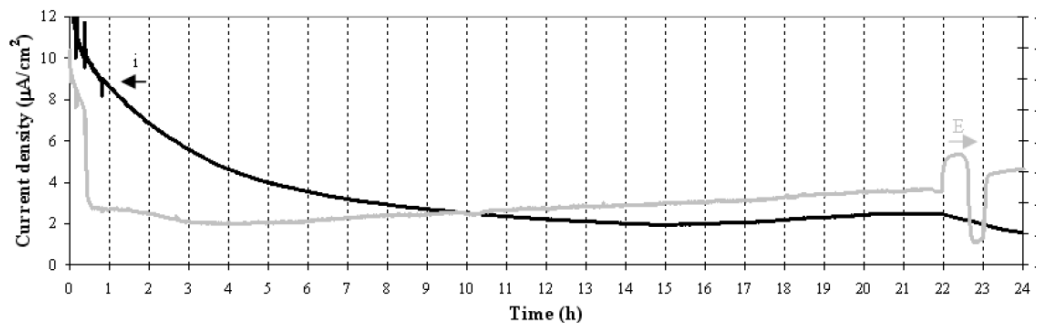
(a) Re = 0
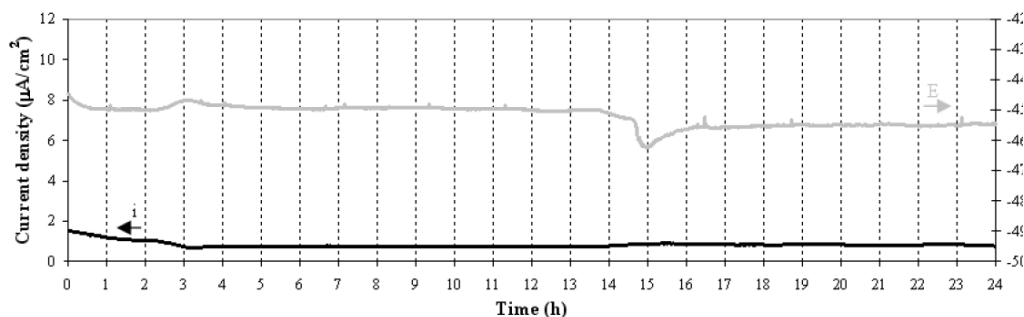
(b) Re = 633
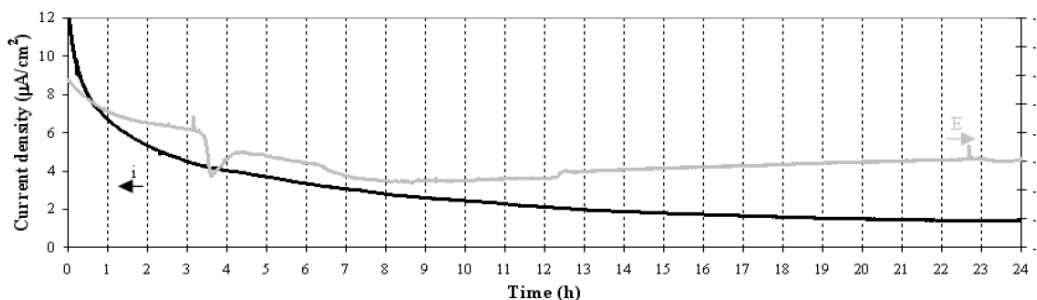
(c) Re = 3166

(d) Re = 5066

Figure 3. Galvanic current density and galvanic potential profiles of the copper/AISI 304 stainless steel pair in an 850 g/L LiBr solution at different Reynolds numbers.

The positive current density values registered indicate that copper is the anodic member of the pair for all the analysed Reynolds numbers; therefore, copper is corroding in all cases, while AISI 304 stainless steel remains protected.

A general tendency for the galvanic current density to decrease with time is observed for all analysed Reynolds numbers. Under stagnant conditions, the galvanic current density decreases during the first three hours and then it stabilizes around 0.80 $\mu A/cm^2$. However, under flowing conditions, the galvanic current density continuously decreases during the 24 hours registered; this decrease is sharp during the first hours but it becomes slower with time, showing a general tendency for the galvanic current density to reach a stable value. The decrease of the galvanic current density with time has also been observed in previous works [37, 38] carried out with a small electrochemical cell in stagnant conditions in LiBr solutions. This decrease of the galvanic current density can be attributed to the formation of a film of corrosion products on the copper surface which grows with time and partially protects this material [37, 39]. With time, the thickness of the corrosion products film increases due to the corrosion process and the diffusion processes go on with more difficulty through the film. From a given time, a steady state can be reached in which the film growth rate is the result of a balance between the separation from the metallic surface of the corrosion products –due to the fluid flow- and the deposition of the new corrosion products formed; this balance can lead to a limiting film thickness and a nearly constant diffusion rate [40]. Therefore, the continuous decrease of the galvanic current density under flowing conditions indicates that the balance between the corrosion products deposition and their separation from the metallic surface due to the fluid flow is favourable to the former during the 24 hours registered; that is, the steady state has not been reached yet, but it seems that the system will reach it soon, practically for all the studied Reynolds numbers.

Figure 3 also shows the galvanic potential profiles. Initially, a general tendency for the galvanic potential to shift to more negative values with time is observed for all analysed Reynolds numbers. Under stagnant conditions, the galvanic potential shifts to more negative values during the first hour and then it seems to stabilize around -450 mV$_{Ag/AgCl}$.; this behaviour coincides with the stabilization of the galvanic current density. However, under flowing conditions, the galvanic potential does not seem to stabilize during the 24 hours registered. Under flowing conditions, the galvanic potential sharply shifts to more negative values during the first hour and then it shifts more slowly to more active potentials; however, from a given hour the tendency of the galvanic potential changes: it shifts slowly to more positive values during the rest of the test. The sharp shift of the galvanic potential to more negative values during the first hour is attributed to the initiation of an active corrosion process; that is, this fact denotes a transitional initial period that indicates the initial activation of the corrosion process when the metal rings get in contact with the lithium bromide solution. This behaviour has also been observed for the corrosion potential in a previous work [41], where the effect of fluid velocity and exposure time on copper corrosion in a concentrated lithium bromide solution was studied. If a sharp shift of the galvanic potential takes place later (during the fifteenth hour for stagnant conditions, during the third and eighth hours for a Reynolds number of 633, at the twenty-second hour for a Reynolds number of 3166 and during the fourth hour for a Reynolds number of 5066), the system tries to recover the previous potential value. The sharp shifts of the potential profiles, in general, are not associated with a significant change in the corresponding galvanic current profiles. These sharp potential shifts to

more negative values are associated with the anodic reaction and the slow potential recoveries in a practically exponential form are associated with the cathodic reaction which restores the electric equilibrium of the system [12]. Finally, the stabilization of the galvanic potential has only been observed under stagnant conditions. However, under flowing conditions, when the galvanic current density begins to decrease more slowly, the galvanic potential begins to shift slowly to less active potentials trying to reach a stable value, just as it happens with the galvanic current density. The general tendency of the galvanic potentials towards more positive values with time is in agreement with the formation of a layer on copper surface.

On the other hand, Figure 3 shows that the galvanic current density and the galvanic potential profiles present very few individual events; this fact is typical in uniform corrosion processes [12]. Moreover, the most remarkable characteristic of uniform corrosion processes is to present potential and current signals with quite low amplitudes [10], like those registered by the copper/AISI 304 stainless steel pair. Figure 4 shows an example of the general amplitude of the signals. The magnitude of the galvanic current density experienced very low oscillations, lower than 0.1 $\mu A/cm^2$, during the 24 hours registered; the magnitude of the galvanic potential also experienced very low oscillations, around 0.2 mV, during the 24 hours registered. Therefore, uniform corrosion could be expected for copper.
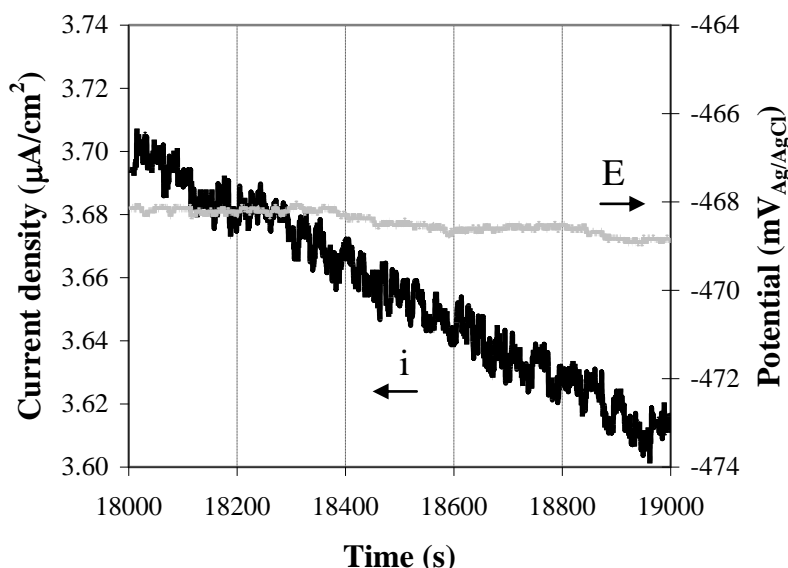

Figure 4. Galvanic current density and galvanic potential profiles of the copper/AISI 304 stainless steel pair at a Reynolds number of 5066 during 1000 s in the sixth hour.

After each experiment, the internal surface of the rings was observed. For all the analysed Reynolds numbers, the copper rings had lost the characteristic initial shine of copper and showed uniform corrosion. This is in agreement with the profiles obtained for the galvanic current density and the galvanic potential. On the other hand, for all the studied Reynolds numbers, the AISI 304 stainless

steel ring surfaces showed no damage. Moreover, the copper rings had lost weight, while the AISI 304 stainless steel rings had not lost any weight. This is in agreement with the positive current density values registered; that is, copper is the anodic member of the pair for all the analysed Reynolds numbers.

3.2. Statistical analysis in the time domain

Besides the visual inspection of the signals registered with time, the statistical analysis of signal fluctuation was performed to obtain the localization index (LI), which could be used to discriminate between different corrosion mechanisms. The mean values of the registered galvanic current density and galvanic potential for each hour of the tests are not presented in this paper because they do not add significant information due to the low amplitudes of the signals (see Figure 4).

The localization index (LI) has been calculated as

$$LI = \sigma_i / i_{rms} \tag{2}$$

where σ_i is the current density standard deviation and i_{rms} is the root mean square of the current density; therefore, LI is always between 0 and 1. Several authors indicate that LI values higher than 0.1 are associated with a typical localized corrosion process, while LI values closer to 0 (lesser than 0.05 or 0.01, depending on authors) are associated with a uniform corrosion process [12, 42]. However, Mansfeld [43] suggests that it is doubtful that a single index derived by statistical methods can identify a certain corrosion mechanism because he calculated LI values for uniform corrosion processes and they were greater than 0.1.
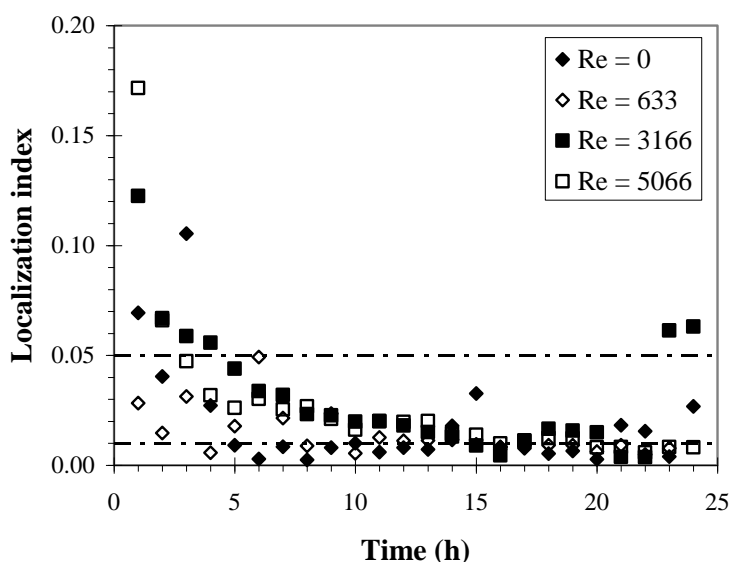

Figure 5. Localization index (LI) values of the copper/AISI 304 stainless steel pair calculated for each hour of the tests at different Reynolds numbers.

Therefore, in this study LI has not been employed as a decisive indicator of the corrosion mechanism, but to confirm the conclusions obtained after the examination of the profiles and the inspection of the ring surface after the tests.

The LI values of the copper/AISI 304 stainless steel pair were calculated for each hour of the tests. Figure 5 shows the values obtained for this index. In general, under both stagnant and flowing conditions, the maximum LI values correspond to the first hours; this fact is probably due to the sharp trend of the experimental data during the first hours of the tests.

The rest of LI values are practically lower than 0.05 at all Re and many of them are close to 0.01, particularly during the last hours of the tests, when the trend of the experimental data is not significant. Therefore, the LI values are much closer to 0.01 than to 0.1 at all studied Reynolds numbers, and according to other authors [12, 42] this fact indicates a uniform corrosion process, thus verifying the results obtained after the examination of the profiles.

3.3. Effect of Reynolds number on galvanic current density and galvanic potential

Figure 6a shows the galvanic current density profiles of the copper/AISI 304 stainless steel pair during 24 h for all the analysed Reynolds numbers. Although the general behaviour of the galvanic current density is similar for all the studied Reynolds numbers (it decreases with time, first more quickly and then more slowly), there are some differences. Under flowing conditions, the galvanic current density values are always greater than under stagnant conditions, as it could be expected, but this difference decreases with time.

On the other hand, under flowing conditions, initially, the galvanic current density is larger for the greatest Reynolds numbers because the effect of increasing fluid velocity is to increase the surface concentration of the corrodent or to decrease the surface concentration of the corrosion products showing a complete or partial mass transfer control [24]; however, with time, the behaviour becomes the opposite: the galvanic current density is larger for the lowest Reynolds number.

This behaviour has also been observed in the corrosion rates in a previous work [41], where the effect of fluid velocity and exposure time on copper corrosion in a concentrated lithium bromide solution was studied. The galvanic current density value is the result of a balance between the separation from the metallic surface of the corrosion products due to the fluid flow and the deposition of the new corrosion products formed.

For the greater Reynolds numbers, the galvanic current density value is the result of a balance between a greater corrosion by a larger fluid velocity and a smaller corrosion due to the formation of a film of corrosion products on copper surface. In other words, for the greater analysed Reynolds numbers, the deposition of corrosion products becomes dominant, because greater quantities of them are initially formed due to a more severe corrosion caused by higher fluid velocity, and subsequently a thicker film is formed.

Mansfeld [1] also attributed the lower galvanic corrosion densities obtained at greater Reynolds numbers to corrosion products deposited on the corroding electrode.
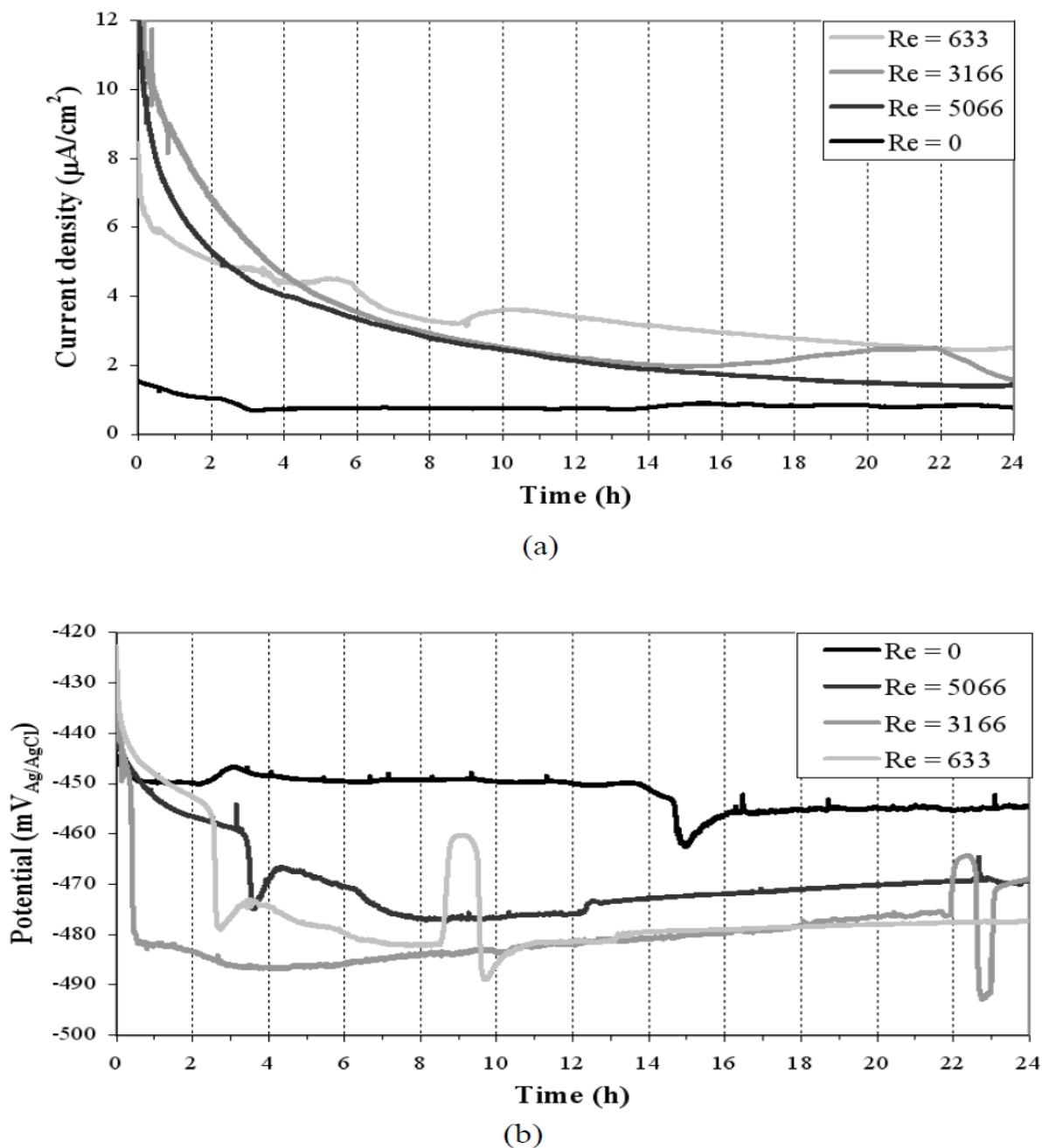
(a)

(b)

Figure 6. Galvanic current density (a) and galvanic potential (b) profiles of the copper/AISI 304 stainless steel pair in an 850 g/L solution for all the analysed Reynolds numbers.

Figure 6b shows the galvanic potential profiles of the copper/AISI 304 stainless steel pair during 24 h for all the studied Reynolds numbers. Although the general behaviour of the galvanic potential is similar for all Reynolds numbers (it sharply shifts to more negative values during the first hour and, from a given hour, it shifts more slowly to more noble potentials with time), there are some differences. After the first hour, the galvanic potential values are always more negative under flowing than under stagnant conditions, showing a more active corrosion process, as it could be expected.

Later, this difference decreases with time (just as it happens with the galvanic current density) because under flowing conditions the galvanic potential begins to shift slowly to less active potentials.

Finally, Table 2 shows that the weight loss of the copper rings agrees with a more severe corrosion under flowing conditions, since a greater weight loss is observed under flowing than under stagnant conditions. On the other hand, the weight loss of the copper rings is not greater as Reynolds number increases and this result agrees with the behaviour of the galvanic current density which is the greatest, with time, at the lowest analysed Reynolds number. Perhaps 24 hours is not a sufficient period of time to appreciate great differences (especially for copper where a film could be formed on it), but the results obtained for the weight loss of copper agree with the galvanic current density profiles obtained. The weight loss of copper for Re = 633 is 2 mg greater than the weight loss of copper for Re = 5066, and the weight loss of copper under flowing conditions is around 5 mg greater than the weight loss of copper under stagnant conditions. There are no great differences in the weight loss values under flowing conditions; similarly, there are no great differences in the galvanic current density profiles obtained under hydrodynamic conditions.

Table 2. Weight loss of copper rings at different Reynolds numbers after 24 hours.

Re	0	633	3166	5066
Weight loss (g)	0.0028	0.0092	0.0072	0.0074

4. CONCLUSIONS

Lithium bromide-water absorption machines powered by solar energy can contribute to the rational utilisation of energy and the protection of the environment. In this work, the influence of Reynolds number on the galvanic corrosion of the copper/AISI 304 stainless steel pair in a concentrated LiBr solution was investigated in a hydraulic circuit using a zero-resistance ammeter (ZRA).

1. Copper is the anodic member of the pair at all analysed Reynolds numbers, and a general tendency of galvanic current density to decrease with time trying to reach a stable value is observed due to the formation of a film of corrosion products on copper surface.

2. The galvanic current density and galvanic potential registered profiles present very few individual events and quite low amplitudes, characteristic of uniform corrosion processes. This fact agrees with the visual inspection of the surface of copper rings after the tests and the localization index values obtained.

3. Under flowing conditions, initially, the galvanic current density increases with Reynolds number, but, with time, this behaviour changes: the galvanic current density is larger at the lowest Reynolds number due to the formation of a thinner film of corrosion products on copper

surface. On the other hand, the galvanic current density values are always greater under flowing than under stagnant conditions. The weight loss of the copper rings agrees with all these results.

References

1. F. Mansfeld, *Corrosion*, 32 (1976) 380.
2. F. Mansfeld and J.V. Kenkel, *Corrosion*, 33 (1977) 236.
3. F. Mansfeld, J.V. Kenkel, *Corrosion*, 33 (1977) 376.
4. R.R. Zahran and G.H. Sedahmed, *Mater. Lett.*, 31 (1997) 29.
5. J.G. Kim, Y.S. Choi, H.D. Lee and W.S. Chung, *Corrosion*, 59 (2003) 121.
6. G. Kear, B.D. Barker, K.R. Stokes and F.C. Walsh, *Corros. Sci.*, 47 (2005) 1694.
7. J.A. Wharton, R.C. Barik, G. Kear, R.J.K. Wood, K.R. Stokes and F.C. Walsh, *Corros. Sci.*, 47 (2005) 3336.
8. C. Wagner and W. Traud, *Zeitschrift fur Elektrochemie und angewandte physikalische Chemie*, 44 (1938) 391.
9. H.P. Hack, *Corrosion: Fundamentals, Testing, and Protection*, Vol 13A, ASM Handbook, ASM International, USA (2003).
10. J.R. Kearns, J.R. Scully, PR. Roberge, D.L. Reichert, J.L. Dawson, *Electrochemical Noise Measurement for Corrosion Applications*, ASTM STP 1227, first ed., Philadelphia (1996).
11. M.G. Pujar, N. Parvathavarthini, R.K. Dayal and H.S. Khatak, *Int. J. Electrochem. Sci.,* 3 (2008) 44-55.
12. F. J. Botana, A. Aballe, M. Marcos, *Ruido Electroquímico. Métodos de análisis*, first ed., Septem Ediciones, Oviedo (2002).
13. J.A. Wharton and R.J.K. Word, *Wear*, 256 (2004) 525.
14. R.J.K. Wood, J.A. Wharton, A.J. Speyer and K.S. Tan, *Tribol. Int.*, 35 (2002) 631.
15. X.Y. Zhou, S.N. Lvov, X.J. Wei, L.G. Benning and D.D. Macdonald, *Corros. Sci.*, 44 (2002) 841.
16. R.A. Cottis, *Corrosion*, 57 (2001) 265-285.
17. *Council Decision of 14 October 1988 concerning the conclusion of the Vienna Convention for the protection of the ozone layer and the Montreal Protocol on substances that deplete the ozone layer*, Official Journal L 297 (1988) 8-28.
18. http://unfccc.int, website of United Nations Framework Convention on Climate Change.
19. G.A. Florides, S.A. Kalogirou, S.A. Tassou and L.C. Wrobel, *Energy Conv. Manag.*, 44 (2003) 2483.
20. R. Fathi and S. Ouaskit, *Rev. Energ. Ren: Journées de Thermique*, (2001) 73.
21. K. Tanno, M. Itoh, T. Takahashi, H. Yashiro and N. Kumagai, *Corros. Sci.*, 34 (1993) 1441.
22. J.W. Furlong, *The Air Pollution Consultant* 11/12 (1994) 1.12-1.14.
23. E. Sarmiento, J.G. González-Rodriguez, J. Uruchurtu, O. Sarmiento and M. Menchaca, *Int. J. Electrochem. Sci.,* 4 (2009) 144-155.
24. T.Y.Chen, A.A. Moccari and D.D. Macdonald, *Corrosion*, 48 (1992) 239.
25. J. Mendoza-Canales and J. Marín-Cruz, *Int. J. Electrochem. Sci.,* 3 (2008) 346-355.
26. A.Y. Musa, A.A.H. Kadhum, A. Bakar-Mohamad, A. Razak-Daud, M. Sobri-Takriff, S. Kartom-Kamarudin and N. Muhamad, *Int. J. Electrochem. Sci.,* 4 (2009) 707-716.

27. S.A.M. Refaey, A.M. Abd El Malak, F. Taha and H.T.M. Abdel-Fatah, *Int. J. Electrochem. Sci.,* 3 (2008) 167-176.
28. M.M. Antonijevic, G.D. Bogdanovic, M.B. Radovanovic, M.B. Petrovic and A.T. Stamenkovic, *Int. J. Electrochem. Sci.,* 4 (2009) 654-661.
29. M.M. Antonijevic, S.C. Alagic, M.B. Petrovic, M.B. Radovanovic and A.T. Stamenkovic, *Int. J. Electrochem. Sci.,* 4 (2009) 516-524.
30. M. Abdallah, M. Al-Agez and A.S. Fouda, *Int. J. Electrochem. Sci.,* 4 (2009) 336-352.
31. C.M. Mustafa and S.M. Shahinoor Islam Dulal, *Corrosion*, 52 (1996) 16.
32. Y. Chen, X.H. Wang, J. Li, J.L. Lu and F.S. Wang, *Electrochim. Acta*, 52 (2007) 5392.
33. E. Zumelzu and C. Cabezas, *J. Mater. Process. Tech.*, 57 (1996) 249.
34. ASTM G-1, *Standard Practice for Preparing, Cleaning and Evaluating Corrosion Test Specimens, ASM International*, USA (1994).
35. ASTM G-5, *Test Method for Making Potentiostatic and Potentiodynamic Anodic Polarization measurements*, ASM International, USA (2004).
36. *Combined Manual for CorrWare and CorrView. Part 1: CorrWare for Windows. Electrochemistry/Corrosion Software. Operating Manual. Version 2.2.* p. 5.14 Scribner Associates, Inc. (2000).
37. E. Blasco-Tamarit, A. Igual-Muñoz, J. García-Antón and D. García-García, *Corros. Sci.*, 50 (2008) 3590.
38. A. Igual-Muñoz, J. García-Antón, J.L. Guiñón and V. Pérez-Herranz, *Corrosion*, 57 (2001) 516.
39. G.T. Burstein, C. Liu and R.M. Souto, *Biomaterials*, 26 (2005) 245.
40. M.T. Montañés, V. Pérez-Herranz, J. García-Antón and J.L. Guiñón, *Corrosion*, 62 (2006) 64.
41. V. Pérez-Herranz, M.T. Montañés, J. García-Antón and J.L. Guiñón, *Corrosion*, 57 (2001) 835.
42. R. Cottis and R. S. Turgoose, *Electrochemical Impedance and Noise in Syrett, B.C. (Eds),Corrosion Testing Made Easy Series*, NACE International, Houston (1999).
43. F. Mansfeld and Z. Sun, *Corrosion*, 55 (1999) 915.